UNIVERSAL INJECTOR AT LERF – BASELINE DESIGN*

S. A. Bogacz†, M. Bruker, J. Grames, J. Gubeli, C. Hernandez-Garcia,
K. Jordan, I. Neththikumara, S. Ogur, T. Satogata, N. Sereno
Thomas Jefferson National Accelerator Facility, Newport News, VA, USA
A. Fomin, Université Paris-Saclay, CNRS/IN2P3, IJCLab, Orsay, France
V. Lizárraga-Rubio, Universidad de Guanajuato, Guanajuato, Mexico

Abstract

A new electron injector complex has been proposed within the Low Energy Recirculating Facility (LERF) vault, which would serve both the 22 GeV CEBAF and the positron programs, while being compatible with the electron source required to produce positrons for Ce$^+$BAF. The baseline design of a 3-pass recirculator features a main linac configured with three cryomodules, five isochronous arcs and three straight sections, allowing electron beam acceleration up to 650 MeV. The injector offers the flexibility to extract 1-pass and 2-pass energy electrons, as needed for positron production, with final reconfiguration to a 3-pass 650 MeV injector for 22 GeV CEBAF. This paper provides an overview of the baseline design of the Universal injector complex, including the 8 MeV injector and the recirculator. A comprehensive suite of beam dynamics studies to validate our design is being launched, starting with start-to-end tracking with Elegant followed by the orbit correction and error mitigation.

LATTICE ARCHITECTURE AND OPTICS

The injector complex [1] is arranged in a racetrack configuration hosting three C-75 cryomodules [2], each containing eight 5-cell cavities operating at 1497 MHz; all three cryomodules are located in a single straight. Starting from an 8 MeV injection energy, the final energy of 650 MeV is reached in three recirculation passes, with each cryo-module providing a 71.3 MeV energy boost. The beam is injected into the racetrack via a three-bend isochronous merger. Five 180° arcs provide recirculation: three on the West side and two on the East side of the racetrack. They are separated vertically by 90 cm (45 cm + 45 cm), with the lowest-energy arcs at the top of the stack. The overall layout is illustrated in Fig. 1. A vertical switch-yard is laid out as a 'three-tier-spreader', initiated by a single vertical bend common to all three passes. The lower-energy spreaders (1st and 2nd pass) are configured as two-step ascents with dispersion suppression in between. The top-energy spreader (3rd pass) features a compact four-point-chicane achromat whose second magnet is shared with the 2nd pass spreader. Recombiners on the East end mirror the spreaders. All arcs employ the Flexible Momentum Compaction (FMC) lattice architecture [3]. The overall optics architecture has been inspired by the PERLE [4, 5] at Orsay.

* This material is based upon work supported by the U.S. DOE, Office of Science, Office of Nuclear Physics contract DE-AC05-06OR23177.
† bogacz@jlab.org

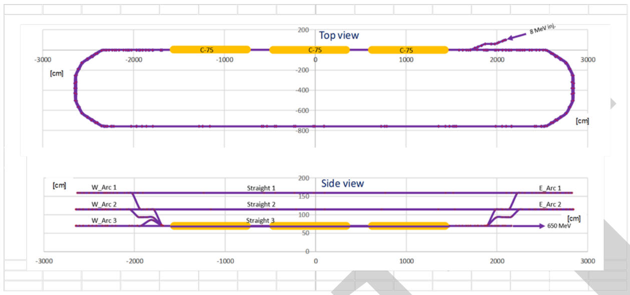

Figure 1: Top and side views of the 3-pass racetrack, featuring vertical stacks of arcs on each side (3 West + 2 East), separated by spreaders and recombiners. The linac, composed of three C-75 cryomodules, achieves a final energy of 650 MeV in three passes.

Merger

Injection at 8 MeV is accomplished through a fixed-field, three-bend merger whose last magnet is placed at the entrance of the linac (Fig. 2). The three-bend configuration and optics architecture, similar to the PERLE [4] design, was chosen for its compactness while maintaining functional modularity. Two quadruplet families flank the merger to provide optimized input/output Twiss functions. The initial quad in the dispersive region, Q1, controls momentum compaction; the subsequent pair Q2 and Q4 closes the achromat; an additional de-focusing quad Q3 at the zero-dispersion crossing balances the beta functions strongly constrained in the horizontal plane. The merger optics (Fig. 3) is tuned to the isochronous condition, yet the architecture also supports non-zero momentum compaction with orthogonal tunability of horizontal dispersion and M_{56}.

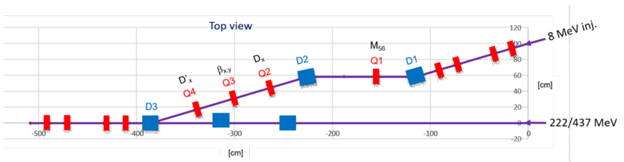

Figure 2: Top view of the 3-bend merger connected to the linac straight, including a re-injection chicane that closes the orbit bump initiated by the last merger bend D3.

Multi-Pass Linac

The last merger bend closes the orbit bump at the lowest injection energy but would deflect higher-pass beams. To suppress the resulting higher-pass bumps, a re-injection chicane is completed by placing two opposing bends upstream

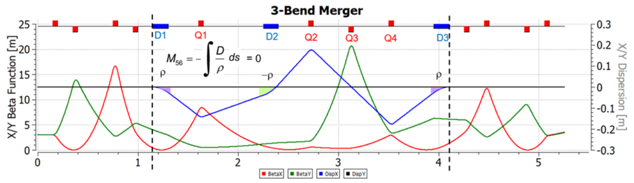

Figure 3: Optics of the 3-bend isochronous merger. Twiss functions at the boundary (dashed lines) are optimized for minimum betas inside the merger.

of the last chicane magnet; these magnets are thus invisible to the 1st-pass beam.

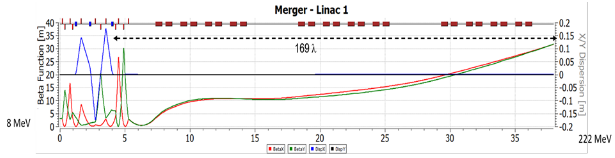

Figure 4: Linac configured with three C-75 cryomodules. The 1st-pass injection optics, tunable via an initial quadrupole quadruplet, is dominated by strong cavity end-field focusing at the front end of the linac.

The multi-pass linac optics is designed as a 'drift linac' with no quadrupoles between the cryomodules. This choice yields quasi-parabolic beta functions that are nearly identical for the 2nd and 3rd passes (Fig. 5); they can be symmetrized across the linac, with maximum beta functions at the linac ends comparable to the linac length of approximately 35 m. This simplifies the overall racetrack architecture and allows nearly identical arcs on both ends of the racetrack.

In contrast, the 1st-pass optics is dominated by cavity end-field focusing (Fig. 4). A weak quadrupole quadruplet is added to provide Twiss flexibility at injection while remaining nearly transparent to the higher passes.

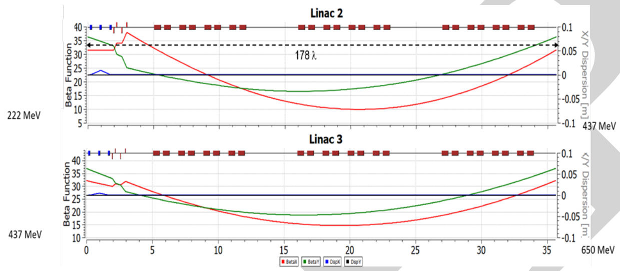

Figure 5: Drift-linac optics for the 2nd and 3rd passes, featuring quasi-parabolic beta functions slightly perturbed by the quadrupole quadruplet.

Recirculating Arcs

The spreaders immediately follow the linac to separate beams of different energies and route them to their respective arcs; recombiners perform the inverse operation before the next linac pass. Each spreader begins with a vertical bending magnet common to all beams. The 1st pass beam steps up 90 cm via a two-step vertical spreader, with three appropriately placed quadrupoles suppressing vertical dispersion between the two steps; this spreader uses four rectangular 30° bends, the first shared with all three passes. The 2nd pass spreader rises by 45 cm in a similar two-step arrangement. The 3rd pass is returned to the linac level by a three-point achromat chicane.

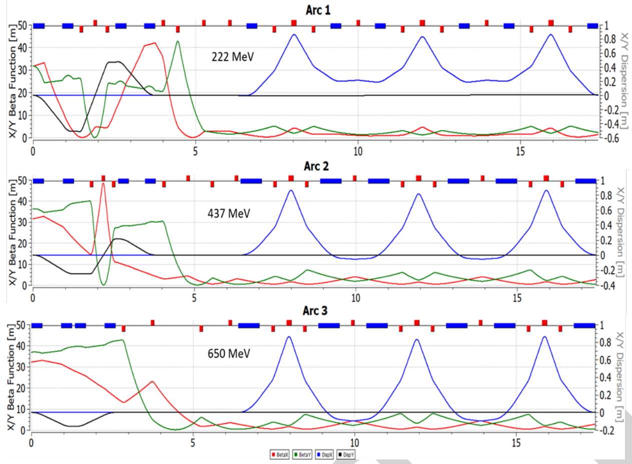

Figure 6: Optics architecture based on the FMC cell. The arcs are tuned to the isochronous condition (net-zero momentum compaction), balancing contributions from horizontal (arc) and vertical (spreader) bends.

Four matching quads follow each spreader to bridge the Twiss functions (two betas and two alphas) between the spreader and the 180° arc. By virtue of the mirror-symmetric higher-pass linac optics, the arcs on the opposite side of the racetrack are simply inverted versions of Arcs 1 and 2.

All five 180° horizontal arcs employ FMC optics (Fig. 6) to allow independent adjustment of the momentum compaction factor in each arc (needed for longitudinal phase-space reshaping). Arc 1 uses six 33 cm sector bends together with two triplets and one singlet; Arcs 2 and 3 use double-length 66 cm sector bends. Consequently, the shorter and longer bends operate at approximately 1.1 T for Arcs 1 and 2, and at 1.65 T for Arc 3. The path length of each arc is chosen to be an integer number of RF wavelengths.

Mirror-Symmetric Straights

The racetrack is completed with three mirror-symmetric straights (Fig. 7): Straight 1 bridges Arc 1 and its East-side mirror; Straight 2 does the same for Arc 2; Straight 3 at top energy terminates at an in-line dump (no Arc 3 exists on the East side). To match the small betas and steep alphas of the arcs, each straight uses a FODO-like structure flanked by two doublets. Lower-energy straights also incorporate path-length correcting doglegs. Each straight contains a single extraction dipole acting as a switch-yard.

Extraction Lines

The Universal Injector provides individual extraction lines for all three passes (Fig. 8). Each line begins with a single bend in the corresponding straight and shares a two-step horizontal jog layout, followed by a replica of the vertical recombiner, which brings all three beams back to the ground-level linac plane (70 cm above the floor).

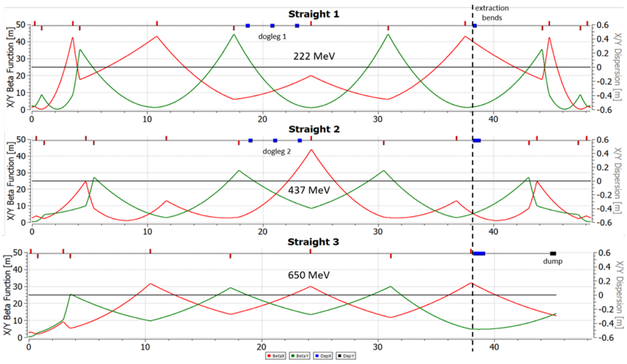

Figure 7: Optics of the mirror-symmetric straights closing the racetrack.

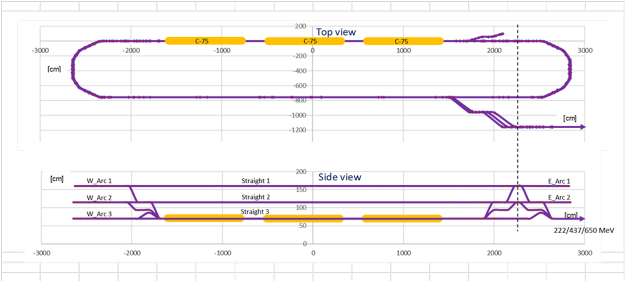

Figure 8: Layout of individual extraction lines featuring a 4 m horizontal jog and a recombiner.

Figures 9 and 10 show detailed magnet layouts and optics of the extraction lines. The 1st, 2nd, and 3rd pass lines use 33 cm, 66 cm, and 99 cm rectangular bends, respectively, while the vertical recombiner replica employs 33 cm rectangular bends throughout.

Figure 9: Individual extraction lines with 33 cm, 66 cm, and 99 cm rectangular bends (blue) for the three energy passes. The vertical recombiner replica uses 33 cm rectangular bends (green).

SUMMARY

A compact injector design within the LERF vault has been presented that serves both the 22 GeV CEBAF [6] and the Ce^+BAF [7] programs. The Universal Injector complex is arranged in a racetrack configuration hosting three C-75 cryomodules. Starting from an 8 MeV merger, a final energy of 650 MeV is reached in three recirculation passes. The injector offers flexible extraction at 1st, 2nd, or 3rd pass energies, as required for positron production and the 22 GeV CEBAF injector.

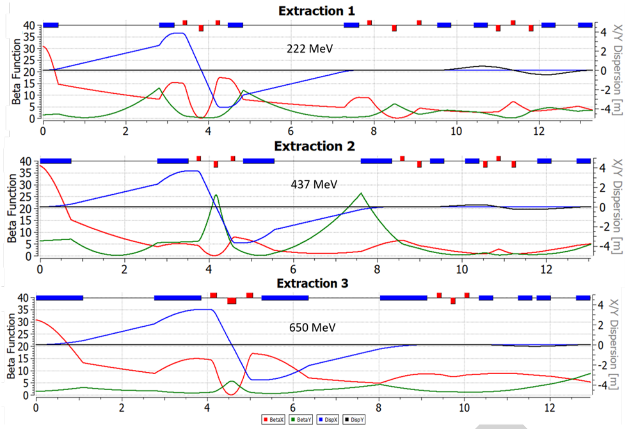

Figure 10: Optics of the individual extraction lines, featuring a 2-step horizontal jog achromat followed by a replica of the vertical recombiner, as in the arcs.

The multi-pass linac optics is configured as a drift linac with no quadrupoles between cryomodules, yielding quasi-parabolic Twiss functions that are nearly identical for both higher passes. All five 180° horizontal arcs employ FMC optics, enabling independent adjustment of the momentum compaction factor in each arc. The presented arc optics architecture offers a high degree of modular functionality for momentum compaction management as well as orthogonal tunability of beta functions and dispersion.

A comprehensive beam dynamics validation program is underway, beginning with the orbit correction scheme and proceeding to start-to-end tracking with lattice misalignment and magnet errors.

ACKNOWLEDGMENT

The authors would like to thank the PERLE Collaboration for sharing concepts and results developed within the project.

REFERENCES

[1] S. A. Bogacz, "Universal injector at LERF – optics design v. 2.0", Jefferson Lab, Newport News, VA, USA, Rep. JLAB-TN-26-026, 2026.

[2] G. Ciovati *et al.*, "Cavity production and testing of the first C75 cryomodule for CEBAF", Jefferson Lab, Newport News, VA, USA, Rep. JLAB-ACC-21-3461, 2021.

[3] D. Douglas, "Flexible Momentum Compaction Lattice Design", Jefferson Lab, Newport News, VA, USA, Rep. JLAB-TN-01-011, 2001.

[4] A. Fomin, private communication, PERLE TDR in preparation.

[5] S. A. Bogacz *et al.*, "Beam dynamics driven design of PERLE", *Phys. Rev. Accel. Beams* no. 27, p. 031603, 2024. doi:10.1103/PhysRevAccelBeams.27.031603

[6] S. A. Bogacz *et al.*, " 22 GeV CEBAF with novel fixed field alternating gradient aesign", in *Proc. SPIN'23 vol. 456*, Durham, NC, USA, Sep. 2023. doi:10.22323/1.456.0145

[7] S. Habet *et al.*, "Concept of a polarized positron source for CEBAF", Jefferson Lab, Newport News, VA, USA, Rep. JLAB-ACC-22-3783, 2022.